ISSN 0038-0946, Solar System Research, 2018, Vol. 52, No. 2, pp. 129–138. © Pleiades Publishing, Inc., 2018.
Original Russian Text © V.V. Shuvalov, V.M. Khazins, 2018, published in Astronomicheskii Vestnik, 2018, Vol. 52, No. 2, pp. 142–151.

Numerical Simulation of Ionospheric Disturbances Generated by the Chelyabinsk and Tunguska Space Body Impacts

V. V. Shuvalov* and V. M. Khazins

Institute of Geosphere Dynamics, the Russian Academy of Sciences, Moscow, 119334 Russia

**e-mail: shuvalov@idg.chph.ras.ru*

Received March 6, 2017

Abstract—Numerical simulation of atmospheric disturbances during the first hours after the Chelyabinsk and Tunguska space body impacts has been carried out. The results of detailed calculations, including the stages of destruction, evaporation and deceleration of the cosmic body, the generation of atmospheric disturbances and their propagation over distances of thousands of kilometers, have been compared with the results of spherical explosions with energy equal to the kinetic energy of meteoroids. It has been shown that in the case of the Chelyabinsk meteorite, an explosive analogy provides acceptable dimensions of the perturbed region and the perturbation amplitude. With a more powerful Tunguska fall, the resulting atmospheric flow is very different from the explosive one; an atmospheric plume emerges that releases matter from the meteoric trace to an altitude of the order of a thousand kilometers.

Keywords: asteroid, comet, asteroid danger, shockwave, meteoric explosion, numerical modeling

DOI: 10.1134/S0038094618010094

INTRODUCTION

One of the detectable and potentially dangerous effects when cosmic body impacts the Earth is generation of large-scale (thousands of kilometers) ionospheric disturbances capable of disrupting the functioning of communication systems. For example, a change in the vertical total electronic content (TEC) by one percent results in a positioning error of several centimeters (Hernández-Pajares et al., 2006). The fall of the Chelyabinsk meteoroid on February 15, 2013, stimulated a new wave of interest in phenomena accompanying the destruction of cosmic bodies in the atmosphere, including effects in the ionosphere. Due to a fairly wide network of ionospheric observation stations, it was possible to detect some disturbances of the ionosphere, which could be related to the fall of the meteoroid (Berngardt et al., 2015), and subsequently to determine the response in the ionosphere in the near zone at distances of 200–300 km from the epicenter using specially developed techniques (Voeykov et al., 2016; Perevalova et al., 2015). Disturbances of the ionosphere were also recorded during the Tunguska catastrophe of 1908 (Ivanov, 1964). In the numerical simulation of shock phenomena, attention is focused on the destruction of and radiation from a cosmic body during its passage through the atmosphere, the propagation of the shock wave along the surface, and the formation of a crater and ejecta from it. Simulation usually concerns the first minutes or seconds after the impact. There are almost no papers describing computer simulation of the generation and propagation of atmospheric disturbances from cosmic body impacts over several hours and for distances of several thousand kilometers. An exception is the recent work (Shuvalov et al., 2017), which presents calculations of ionospheric disturbances after the hypothetical fall of the Apophis asteroid.

The purpose of this paper is to simulate ionospheric disturbances caused by the two most famous terrestrial impact events in the last 150 years: the fall of the Chelyabinsk and Tunguska space bodies (hereinafter referred to as CSB and TSB).

CALCULATION METHOD

The initial impact stage, destruction and deceleration of the cosmic body in the atmosphere were calculated by the model (Shuvalov, Artemieva, 2002; Artemieva, Shuvalov, 2016; Shuvalov et al., 2016), which considers deformation of a completely destroyed meteoroid under the impact of an aerodynamic load, its vaporization by shock-heated air radiation, fragmentation and conversion into a retarding gas jet with small fragments. The results of these calculations serve as initial data for the three-dimensional SOVA program (Shuvalov, 1999a), which is used to calculate ionospheric disturbances. At ionospheric altitudes, dissipative processes, viscosity, and thermal conductivity, which are usually neglected at low altitudes (up to 100 km), can play an important

role. Therefore, the Euler equations in the SOVA program were replaced by the Navier–Stokes equations to calculate the atmospheric flows. Thermal conductivity was also taken into account in a number of two-dimensional calculations, but it did not contribute significantly to the solution, therefore, the thermal conductivity was not taken into account in the three-dimensional calculations. Some two-dimensional variants were calculated from a different gas-dynamic model based on the flow correction method in order to control the adequacy of the model used (Khazins and Shuvalov, 2016).

A very detailed difference grid of 800 points vertically and 3200 points horizontally was used in two-dimensional calculations, while the three-dimensional calculations were coarser: 400 vertical (Z) and horizontal (X) points, and 190 points in Y-direction perpendicular to the vertical plane in which the trajectory of the incident body lies.

In a dissipative atmosphere, the molecular viscosity coefficient can be written in the form (Huang et al., 2014):

$$\mu = 3.54 \times 10^{-7} (T^*)^{0.69}.$$

The units of μ are kg m^{-1} s^{-1}. Tables (Kuznetsov, 1965) were used as an equation of state, which us allow to satisfactorily describe both the high-temperature and low-temperature regions. Such a description of the characteristics of the medium is valid up to altitudes on the order of 100 km; at higher altitudes, they are correct only in the first approximation, since the air composition begins to change at those altitudes.

The condition of nonflow (a rigid wall) was set at the lower boundary of the computational domain. At the lateral boundaries, background conditions were set, however, a doubling was performed and the boundaries were moved away when the disturbances reached the lateral boundary (along X or Y). The same was done with the upper boundary. Formally, the approximation of gas dynamics and, accordingly, the model that we use works up to an altitude of about 400 km. At this altitude, the particles' passages in the undisturbed atmosphere are compared with the characteristic altitude of the atmosphere. We considered three possible boundary conditions on the upper boundary. The first is that the calculation area is formally extended up to the altitudes where the equations of gas dynamics no longer work. This leads to the fact that very strong disturbances develop at elevations of more than 400 km, which greatly limits the time step and, accordingly, increases the calculation time. The second method consists in using Rayleigh viscosity (Xu et al., 2003) at altitudes of more than 400 km, which leads to attenuation of disturbances in the region where gas dynamics do not work. In this case, problems with density arise at the stage when the ejected dense material starts to fall under the action of gravity. And, finally, the third option, the most successful from our point of view, is to periodically (carried out once per hundred calculated layers) fill regions where the density is lower than the equilibrium density at an altitude of 500 km with fixed background. All three boundary conditions hardly affect the flow at altitudes of 200–300 km, but the latter provides a minimum calculation time.

IONOSPHERIC DISTURBANCES GENERATED BY THE CHELYABINSK EVENT

Figure 1 presents the numerical results for the initial stage of ionospheric disturbances after the CSB impact. Three options were considered. In the first case, a dunite meteoroid with a diameter of 19 m and density of 3.3 g/cm^3 fell at an angle of 19° at a speed of 20 km/s. In the second case, the same meteoroid fell vertically. The third option is an explosion with a capacity of 500 kt of TNT equivalent (about the same as the energy of a meteoroid) at an altitude of 20 km. The main difference between these cases is that in the first two cases, the energy release zone has an elongated shape. The main energy is released near the deceleration point, but there is an extended rarified channel above it that expands and generates a shock wave.

At time 30 s, the atmospheric flows in different cases greatly differ from each other. This difference is maintained even 150 seconds after the energy release. But after 360 s, all the flows become similar to each other and look like a typical flow caused by a spherical explosion. The flows generated by the meteoroid impacts (the first two cases) develop a little faster than a purely explosive flow.

To estimate the atmospheric disturbances at a fixed point in space, we introduce the quantity $\in = \max(abs((\rho - \rho_0)/\rho_0))$, that characterizes the maximum amplitude of density oscillations at this point. Here, $\rho_0(z)$ is the equilibrium air density in the atmosphere at an altitude z. A grid of fixed marker points (on the order of a million points) is introduced in the entire calculation area. The value $abs((\rho - \rho_0)/\rho_0)$ is calculated and its maximum value (i.e., $\in$) is retained at each of these points, at each time step.

It can be seen from Fig. 2 that all three considered options give spatial distributions of the maximum density oscillation amplitude $\in$ that are not very different. The size of the region where density disturbances at altitudes of 200–300 km exceed 5% reaches 3000–4000 km, while at distances of up to 500 km from the epicenter the ionospheric density disturbance is 20% or more. The slope of the trajectory leads to some horizontal displacement and a slight decrease in the disturbed region. To estimate the effect of specific weather conditions, calculations of explosion were performed with two different atmospheric models: the standard CIRA (CIRA, 1961) and one corresponding to the time and place of the Chelyabinsk event obtained using the MSIS-90 model (Hedin, 1991). The difference between the explosion calculation

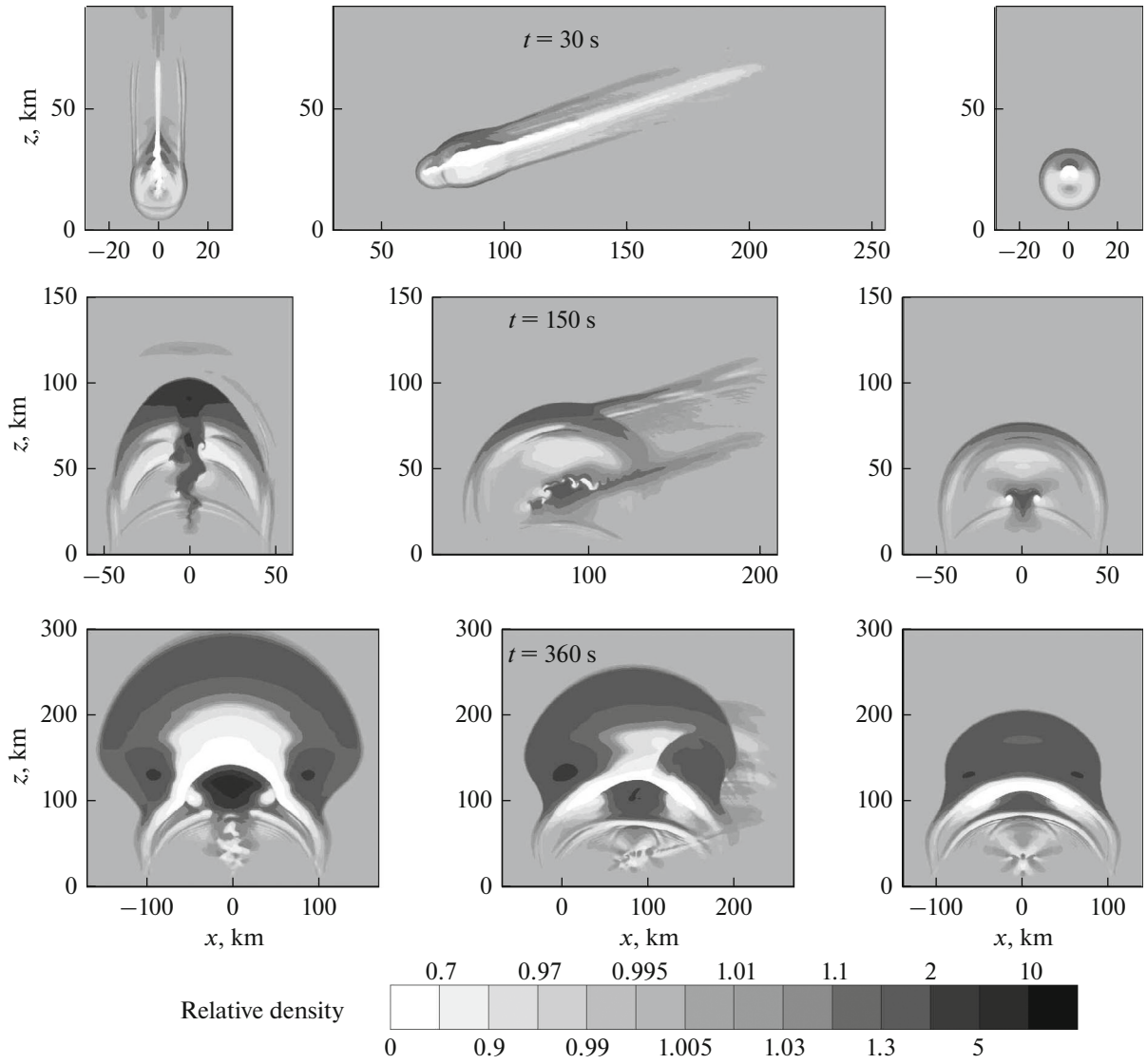

Fig. 1. Relative air density ρ/ρ_0 distributions in 30, 150, and 360 s after the deceleration of the Chelyabinsk space body. The vertical fall of the meteoroid is on the left, an explosion at an altitude of 20 km is on the right, a meteoroid with an entrance at an angle of 19° is in the center.

results with different atmospheric models (see Fig. 2) is approximately the same as the difference between the results of the explosion calculation and the total impact problem. Apart from the cases described above, an explosion with an energy of 500 kt at an altitude of 30 km was simulated; the $\in$ distributions differ from those considered above just slightly.

As can be seen from Fig. 1, the Chelyabinsk meteoroid energy release differs significantly from the axisymmetric one. However, after about 10 minutes (Fig. 1), the disturbed ionosphere region acquires an almost axisymmetric form, and the total pictures of ionospheric disturbances in the explosion and oblique impact differ little (see Fig. 2). Based on this, we compared the observation data with the calculations of the disturbances generated by the CSB for the third case (the calculation of which takes the least time), i.e., in the approximation of instantaneous energy release in an axisymmetric region.

A common characteristic of ionospheric disturbance is the deviation dI of the total electron content (TEC) in the path of the beam from the background TEC value. The Chelyabinsk event occurred on February 15, 2013, at 03:20 UT, that is, near the boundary of the solar terminator, separating the low night values of the background electron concentration from the daytime values.

Figure 3a shows the distribution of the background concentration at two moments of time, obtained with the IRI-2012 model (Bilitza et al., 2014). The difference between the daytime and morning values of the background electron concentration reaches a factor of

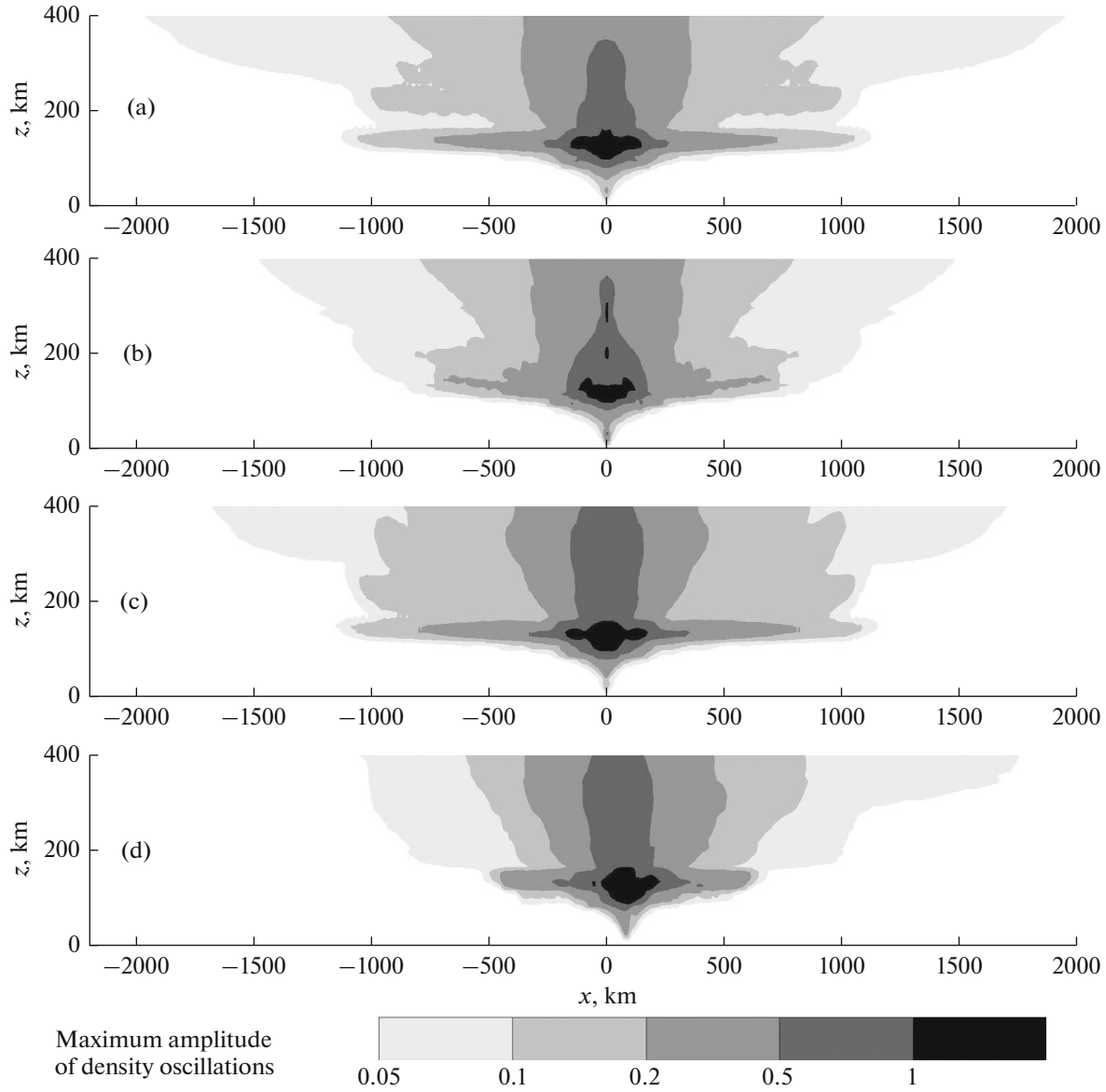

Fig. 2. Distributions of the maximum amplitude of density fluctuations $\in$, for different cases: (a) spherical explosion in the CIRA atmosphere, (b) spherical explosion in the MSISE atmosphere, (c) vertical meteoroid fall, (d) meteoroid fall at an angle of 19º.

five. In the calculations, we used a time-invariant distribution at time 03 UT. Figure 3b shows the dI distribution in the units of total electronic concentration TECU (1 TECU = 10^{16} electron/m^2) obtained as a result of numerical simulation by calculating the corresponding integrals along the vertical beam at a distance of 300 km from the axis of symmetry. The results of vertical sounding obtained by processing observational data from one of the Arti geophysical observatory stations located about 250 km from the place of the meteor explosion (Perevalova et al., 2015) are also given there. As can be seen, there is good agreement between observational and calculated data on the amplitude and period. At the same time, the calculated signal begins with a positive phase, and not a negative one, as follows for a given localization of observations. The work (Gokhberg et al., 2013) pays attention to formation of the negative phase of the signal, the so-called inverted N-wave. A study of the TEC variations that were initiated by a series of the strongest underwater earthquakes leads M.B. Gokhberg and coauthors (Gokhberg et al., 2014) to the conclusion that the anisotropy of the medium generated by the geomagnetic field is responsible for the formation of a particular N-wave phase. In the present work, the impact of geomagnetic field is not taken into account.

The presented comparison of calculated and observational data indicates the consistency of numerical simulation with the real processes.

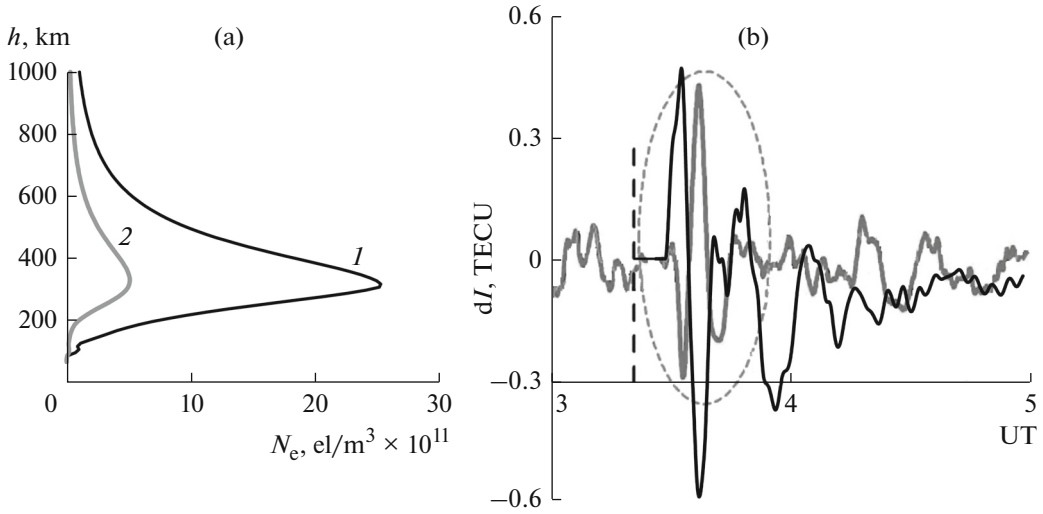

Fig. 3. (a) Background electron concentration: 15.02.2013, 9UT (*1*); 15.02.2013, 3UT (*2*). (b) Total electron content. The gray curve is the published results of the TEC time distribution in the south-west direction from the place of the "meteoric explosion" (Perevalova et al., 2015); the black curve is the result of numerical TEC simulation.

Based on comparisons of ionospheric disturbances generated by TNT explosions with a power of 0.26–2 kt with disturbances recorded upon the fall of the Chelyabinsk meteoroid Ruzhin et al. (2014) conclude that there is possibly a significant overestimation in the TNT equivalent of the Chelyabinsk event in existing publications. The authors see one of the possible reasons for this discrepancy in the difference between the energy release during an explosion and the braking of a meteoroid. Our calculations and results of simulation published in (Popova et al., 2013) show that both atmospheric disturbances and excess pressures on the Earth's surface depend relatively weakly (by no more than 2–3 times) on the method of energy release. Apparently, the reason must be sought in something else.

IONOSPHERIC DISTURBANCES GENERATED BY THE TUNGUSKA EVENT

The atmospheric flow arising from the fall of the Tunguska cosmic body differs significantly from that considered above. This difference is due to the role of the atmospheric trail formed during the flight of the cosmic body through the atmosphere. In the study of Shoemaker-Levy 9 comet's fragments fall to Jupiter (Boslough and Crawford, 1997) it was found that the presence of a trail can lead to formation of an atmospheric plume that rises up along the trail and throws a denser gas from the lower layers of the atmosphere into the thinner upper atmosphere. The mechanism of plume formation due to perturbation of hydrostatic equilibrium in a rarefied meteor trail was considered in detail in the paper (Shuvalov, 1999b), where it was shown that plumes appear when large enough bodies (diameter > 50 m) fall. In the case of smaller bodies (≤10–20 m), a plume does not have time to develop because of mixing of the trail with the surrounding air due to the development of the Kelvin-Helmholtz instability at the boundaries of the trail.

The formation of the plume is clearly visible in Fig. 4, which shows the initial stage of formation of ionospheric disturbances in one of the possible scenarios of the Tunguska catastrophe, namely, when a comet with a diameter of 80 m falls at a speed of 30 km/s at an angle of 45 degrees.

At 7 s, the gas begins to accelerate upward along the trail in the entire rarified trail. The density of the gas (a mixture of air and vapor) throughout the trail is less than the equilibrium atmospheric density, while the pressure gradient is greater, because the pressure itself is greater than outside the track. The maximum pressure gradients (both in the trail and outside it) are observed at low altitudes (below the mesopause), where the gas accelerates faster and—colliding with a slower gas rising above the mesopause—generates a shock wave that is clearly visible in it at time 50 s. Gas accelerated inside the trail rises upward, into more rarified layers, becomes heavier than the ambient air, but continues to fly upwards by inertia, i.e., a plume is formed. At altitudes of about 1500 km, the plume slows in the gravity field and begins to descend; oscillatory movements occur (see Fig. 7).

Further evolution of ionospheric disturbances is shown in Fig. 5. The rise of the plume, its fall, and subsequent fluctuations are accompanied by the generation and vertical propagation of shockwaves that gradually translate the energy of the plume into heat. The heated region of the atmosphere in the region of the "explosion" expands sideways, generating a shock wave in front of it. For comparison, Fig. 5 shows the distribution of density perturbations in the atmo-

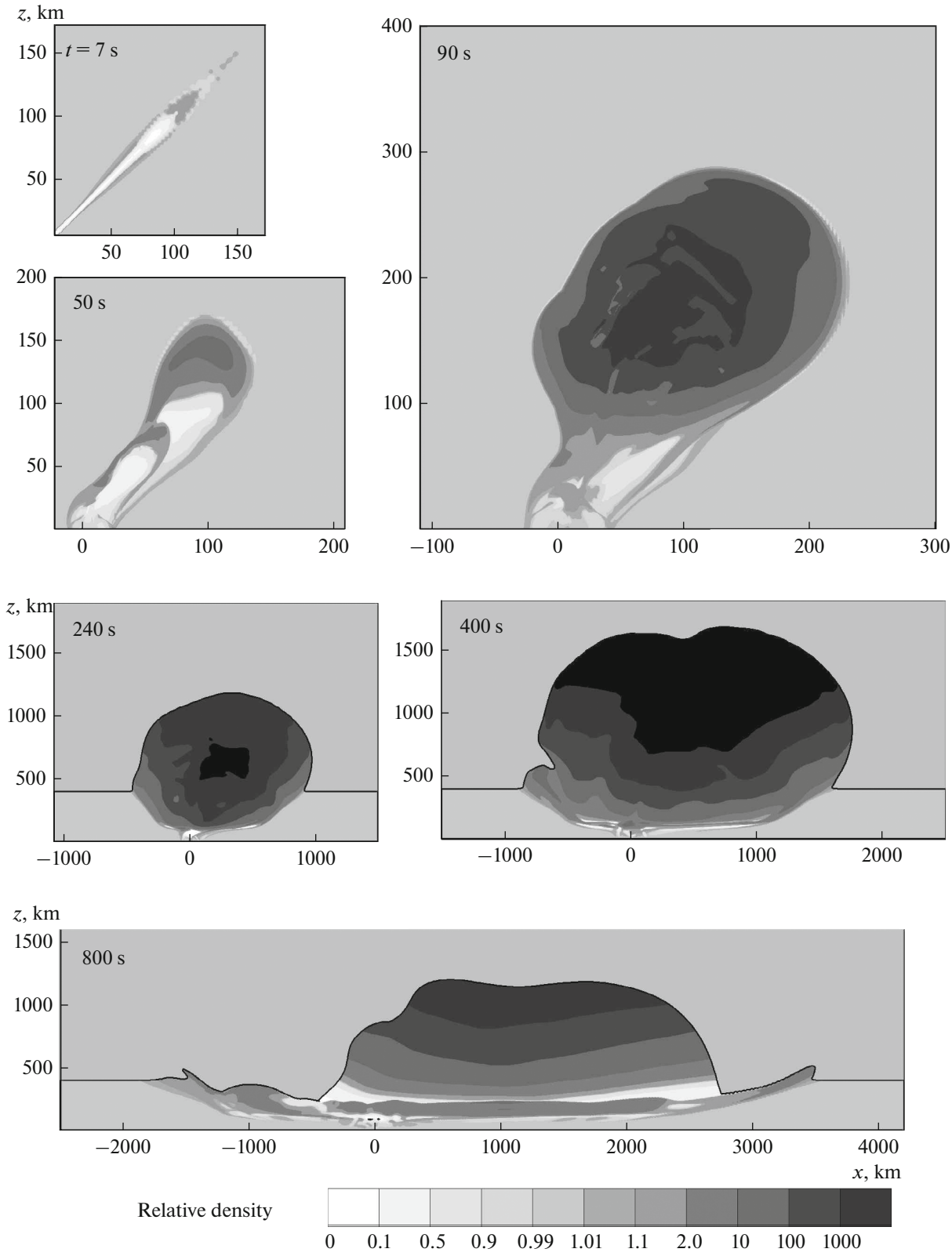

Fig. 4. The initial stage of the formation of ionospheric disturbance after impact of a comet with a diameter of 80 m at a speed of 30 km/s at an angle of 45°. The black line shows the density contour corresponding to a value of 5×10^{-15} g/cm^3 (equilibrium density at an altitude of 400 km). Areas where the density is less than 5×10^{-15} g/cm^3 and where the gas-dynamic approximation does not work are shaded with a gray background color.

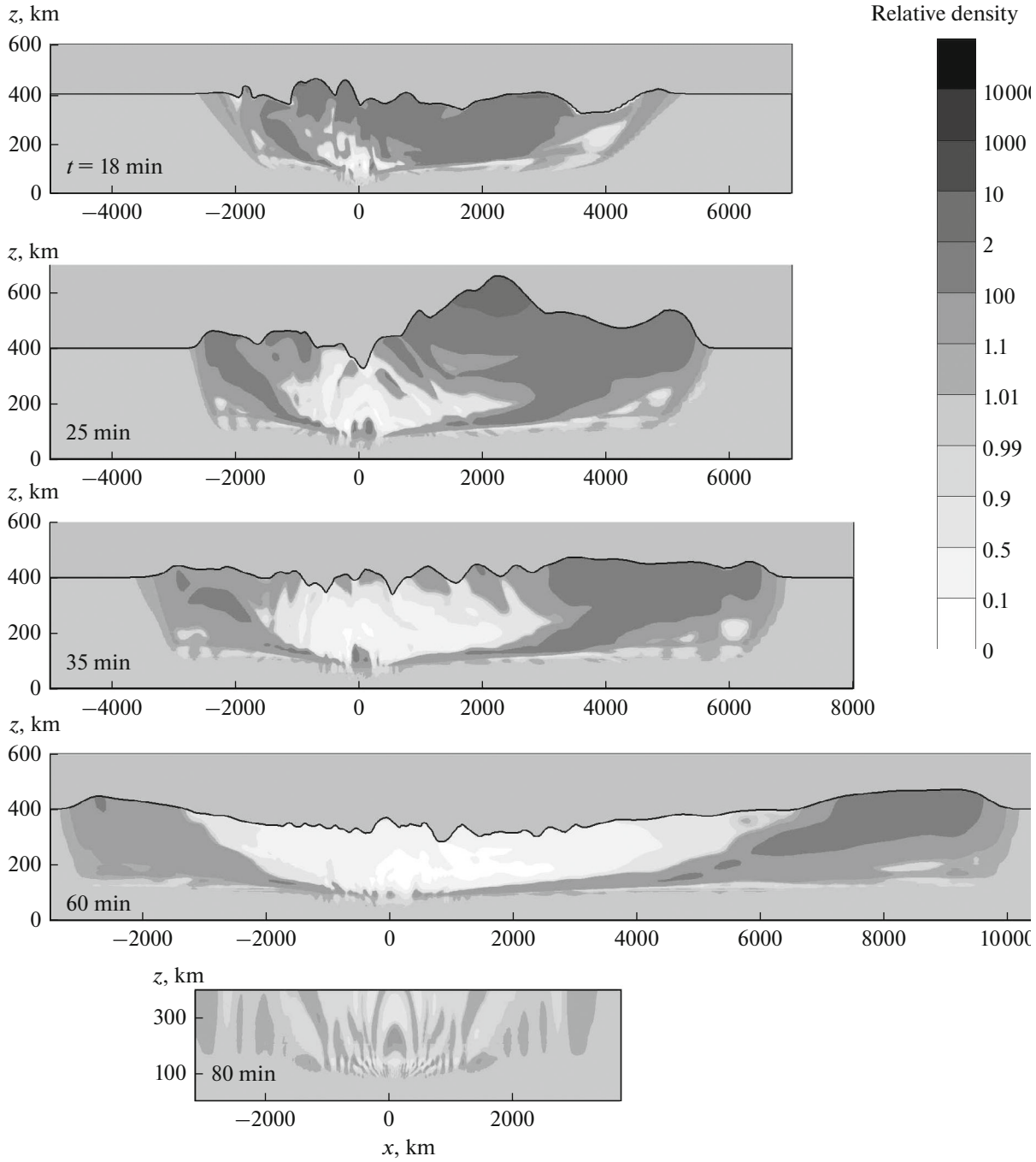

Fig. 5. Propagation of ionospheric disturbances during the first hour after the fall of a comet with an 80 m diameter at a speed of 30 km/s at an angle of 45°. The black line shows the density contour corresponding to a value of 5×10^{-15} g/cm^3 (equilibrium density at an altitude of 400 km). Areas where the density is less than 5×10^{-15} g/cm^3 and where the gas-dynamic approximation does not work are shaded with a gray background color. For comparison, the atmospheric disturbances in 80 minutes after the CSB impact is shown on the same scale in the lower figure. Vertical and horizontal scale differ by a factor of 4.

sphere 80 minutes after the fall of the CSB, demonstrating a qualitative difference between the natures of atmospheric disturbances in these two cases.

Density perturbations in the ionosphere caused by the Tunguska catastrophe are much stronger than in a spherical explosion with an energy equal to the kinetic energy of the TSB at an altitude of 10 km (see Fig. 6). They are about an order of magnitude greater than the ionospheric disturbances caused by the fall of the Chelyabinsk meteorite. The calculations were finished at a time of 100 min (6000 s), when the characteristic radius of the perturbed region became comparable to

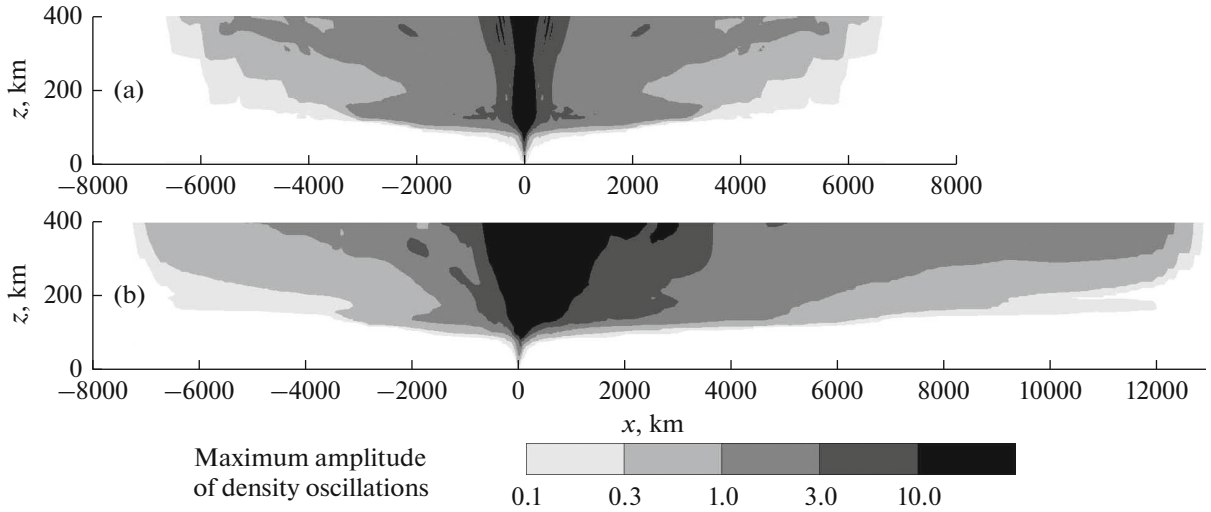

Fig. 6. Distributions of the maximum amplitude of density oscillations ∈ for a spherical explosion with an energy of 13 Mt at an altitude of 10 km and for a comet impact with a diameter of 80 m at a speed of 30 km/s at an angle of 45° (with the same energy of 13 Mt).

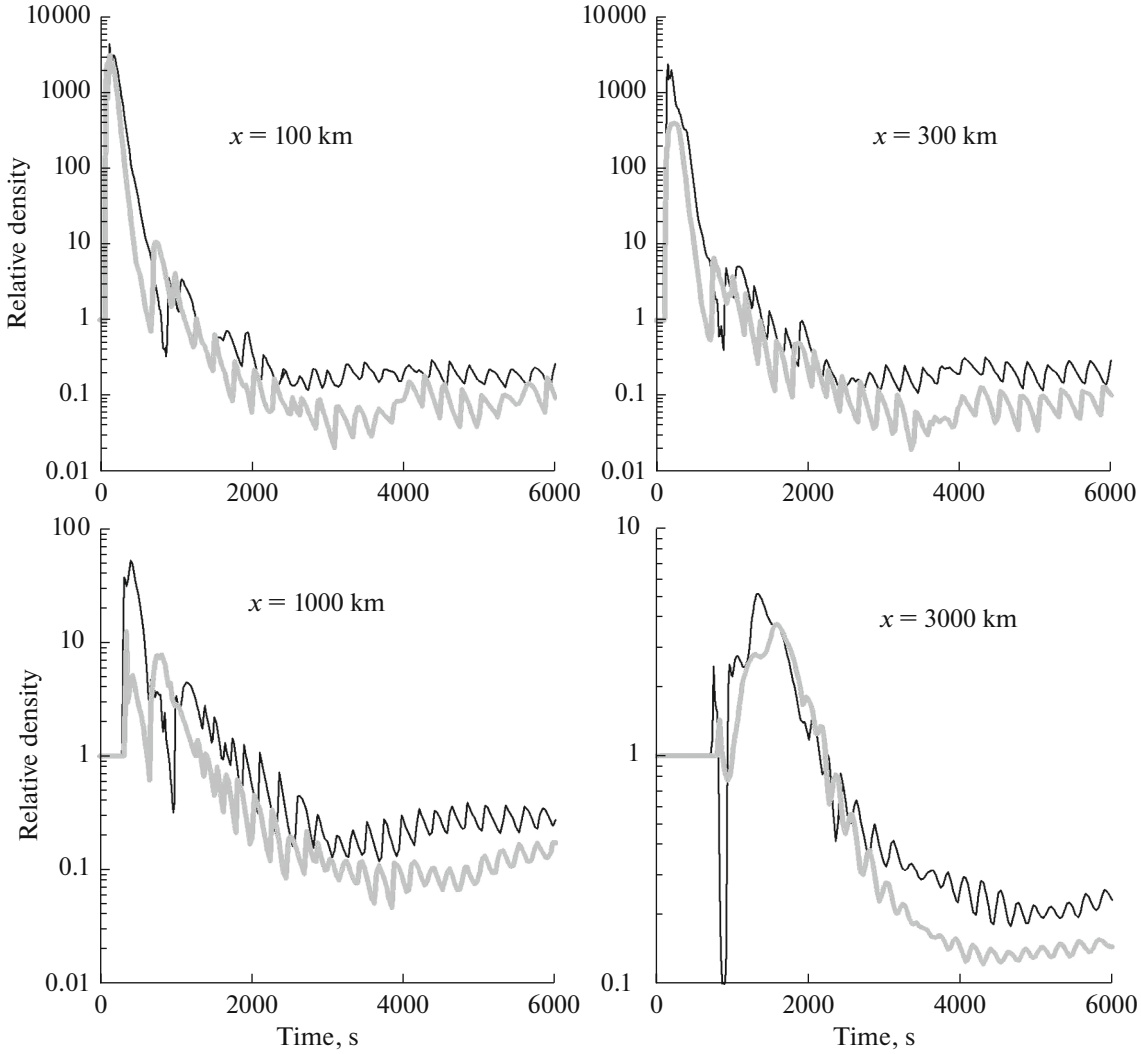

Fig. 7. Relative density $\rho/\rho_0(z)$ dependence on time at altitudes of 200 km (gray line) and 300 km (black line) at different distances *X* from intersection of the CSB trajectory with the Earth's surface.

the Earth's radius. At large distances, the sphericity of the Earth, which we did not take into account, is already significant. At the time the calculations are concluded, the perturbation region with a value $\epsilon > 1$ has already reached its maximum size; the region of weaker perturbations still continues to increase. Taking into account the sphericity of the Earth will contribute to this increase.

In both cases, with the fall of the Tunguska and Chelyabinsk cosmic bodies, atmospheric disturbances are concentrated at altitudes of more than 100 km, where the characteristic altitude of the atmosphere is several tens of kilometers. At altitudes below 100 km, the perturbations decay quickly due to a very strong density gradient (a small characteristic altitude of the atmosphere).

Time dependences of the relative density at different altitudes and different distances from the impact epicenter (see Fig. 7) show that higher frequency density perturbations with a characteristic period of 200–250 s are observed against the background of large-scale (with a characteristic size of thousands of kilometers and a period of more than an hour) density perturbations that are clearly visible in Fig. 5. Oscillations of approximately the same frequency are also observed during the CSB fall.

CONCLUSIONS

Calculations of ionospheric disturbances caused by the fall of the Chelyabinsk meteoroid in three approximations were performed. In the first one, the velocity and thermodynamic quantity distributions obtained from the simulation of deceleration of a meteoroid falling at an angle of 19° were used as the initial data. In the second case, the results of calculation of a vertical meteoroid fall were taken as the initial data. In the third (simplest) approximation, a spherical explosion with an energy equal to the kinetic energy of a meteoroid at altitudes of 20 and 30 km was considered. Comparison of the results obtained in different approximations showed that the difference between them is approximately the same (20–40%) as the one introduced by uncertainty in distribution of atmospheric parameters at the time of impact. Based on this, we can conclude that if we want to construct a model of a specific meteor phenomenon for which atmospheric parameter distributions at the time of impact are known, then it is better to solve the complete problem of the meteoroid entering the atmosphere and the subsequent propagation of perturbations. If, however, we want to predict atmospheric disturbances caused by the impact of a cosmic body of a certain size that will drop at an unknown time and location, then in the first approximation one can regard the impact as a spherical explosion. This conclusion is correct only for the fall of relatively small meteoroids (20–30 m and less). For impacts of larger bodies, for example, the Tunguska cosmic body, the picture of the atmospheric flow is qualitatively different; the role of the meteoric trail increases and an atmospheric plume is formed that emits dense air from the lower dense layers of the atmosphere to great altitudes. The spherical explosion model works poorly in this case.

ACKNOWLEDGMENTS

This work was supported by the Russian Science Foundation (grant no. 16-17-00107). The authors are grateful to the reviewers for the careful reading of the work and valuable comments.

REFERENCES

Artemieva, N.A. and Shuvalov, V.V., From Tunguska to Chelyabinsk via Jupiter, *Annu. Rev. Earth Planet. Sci.*, 2016, vol. 44, pp. 37–56.

Berngardt, O.I., Perevalova, N.P., Kutelev, K.A., Zherebtsov, G.A., Dobrynina, A.A., Shestakov, N.V., Zagretdinov, R.V., Bakhtiyarov, V.F., and Kusonsky, O.A., Toward the azimuthal characteristics of ionospheric and seismic effects of "Chelyabinsk" meteorite fall according to the data from coherent radar, GPS, and seismic networks, *J. Geophys. Res.*, 2015, vol. 120, no. 12, pp. 10754–10771.

Bilitza, D., Altadill, D., Altadill, D., Zhang, Y., Zhang, Y., Mertens, C., Mertens, C., Truhlik, V., Truhlik, V., Richards, P., Richards, P., McKinnell, L.-A., McKinnell, L.-A., and Reinisch, B., The International Reference Ionosphere 2012—a model of international collaboration, *J. Space Weath. Space Clim.*, 2014, vol. 4, no. A07, p. 12.

Boslough, M.B. and Crawford, D.A., Shoemaker-Levy 9 and plume-forming collisions on Earth, *Proc. United Nations Int. Conf. "Near-Earth Objects,"* Remo, J.L., Ed., New York: NY Acad. Sci., 1997, pp. 236–282.

CIRA, *COSPAR International Reference Atmosphere*, Amsterdam: North Holland, 1961.

Gokhberg, M.B., Ol'shanskaya, E.V., Steblov, G.M., and Shalimov, S.L., The Chelyabinsk meteorite: Ionospheric response based on GPS measurements, *Dokl. Earth Sci.*, 2013, vol. 452, no. 1, pp. 948–952.

Gokhberg, M.B., Ol'shanskaya, E.V., Steblov, G.M., and Shalimov, S.L., The ionospheric response to the acoustic signal from submarine earthquakes according to the GPS data, *Izv. Phys. Solid Earth*, 2014, vol. 50, no. 1, pp. 1–8.

Hedin, A.E., Extension of the MSIS thermosphere model into the middle and lower atmosphere, *J. Geophys. Res.: Space Phys.*, 1991, vol. 96, no. 2, pp. 1159–1172.

Hernández-Pajares, M., Juan, J.M., and Sanz, J., Medium-scale traveling ionospheric disturbances affecting GPS measurements: Spatial and temporal analysis, *J. Geophys. Res.*, 2006, vol. 111, pp. 1–13.

Huang, K.M., Zhang, S.D., Yi, F., Huang, C.M., Gan, Q., Gong, Y., and Zhang, Y.H., Nonlinear interaction of gravity waves in a nonisothermal and dissipative atmosphere, *Ann. Geophys.*, 2014, vol. 32, pp. 263–275.

Ivanov, K.G., Geomagnetic effect of the Tunguska meteorite fall, *Meteoritika*, 1964, no. 24, pp. 141–151.

Khazins, V.M. and Shuvalov, V.V., Numerical modeling of acoustic-gravitational waves initiated by the fall of a meteoroid, in *Dinamicheskie protsessy v geosferakh* (Dynamic Processes in Geospheres), Nauch. Tr. Inst. Din. Geosfer, Ross. Akad. Nauk, Moscow: GEOS, 2016, no. 8, pp. 197–207.

Kuznetsov, N.M., *Termodinamicheskie funktsii i udarnye adiabaty vozdukha pri vysokikh temperaturakh (Thermodynamic Functions and Impact Adiabats of Air at the High Temperatures)*, Moscow: Mashinostroenie, 1965.

Perevalova, N.P., Shestakov, N.V., Voeykov, S.V., Takahashi, H., and Guojie, M., Ionospheric disturbances in the vicinity of the Chelyabinsk meteoroid explosive disruption as inferred from dense GPS observations, *Geophys. Res. Lett*., 2015, vol. 42, pp. 6535–6543.

Popova, O.P., Jenniskens, P., Emel'yanenko, V., Kartashova, A., Biryukov, E., Khaibrakhmanov, S., Shuvalov, V., Rybnov, Y., Dudorov, A., Grokhovsky, V.I., Badyukov, D.D., Yin, Q.-Z., Gural, P.S., Albers, J., Granvik, M., et al., Chelyabinsk airburst, damage assessment, meteorite recovery, and characterization, *Science*, 2013, vol. 342, no. 6162, pp. 1069–1073.

Ruzhin, Y.Y., Kuznetsov, V.D., and Smirnov, V.M., Ionospheric response to the entry and explosion of the South Ural superbolide, *Geomagn. Aeron*., 2014a, vol. 54, no. 5, pp. 601–612.

Ruzhin, Yu.Ya., Kuznetsov, V.M., and Smirnov, V.M., The ionosphere effects of the Chelyabinsk meteoroid explosion, *Int. J. Electron. Appl. Res*., 2014b, vol. 1, no. 2, pp. 39–60.

Shuvalov, V.V., Multi-dimensional hydrodynamic code SOVA for interfacial flows: application to thermal layer effect, *Shock Waves*, 1999a, vol. 9, no. 6, pp. 381–390.

Shuvalov, V.V., Atmospheric plumes created by meteoroids impacting the Earth, *J. Geophys. Res.: Planets*, 1999b, vol. 104, no. 3, pp. 5877–5890.

Shuvalov, V.V. and Artemieva, N.A., Numerical modeling of Tunguska-like impacts, *Planet. Space Sci*., 2002, vol. 50, pp. 181–192.

Shuvalov, V.V., Popova, O.P., Svettsov, V.V., Trubetskaya, I.A., and Glazachev, D.O., Determination of the height of the "meteoric explosion," *Sol. Syst. Res*., 2016, vol. 50, no. 1, pp. 1–12.

Shuvalov, V.V., Svettsov, V.V., Artem'eva, N.A., Trubetskaya, I.A., Popova, O.P., and Glazachev, D.O., Asteroid Apophis: evaluating the impact hazards of such bodies, *Sol. Syst. Res*., 2017, vol. 51, no. 1, pp. 44–58.

Voeykov, S.V., Berngardt, O.I., and Shestakov, N.V., Use of the index of TEC vertical variation disturbance in studying ionospheric effects of the Chelyabinsk meteorite, *Geomagn. Aeron*., 2016, vol. 56, no. 2, pp. 219–228.

Xu, J., Smith, A.K., and Ma, R., A numerical study of the effect of gravity-wave propagation on minor species distributions in the mesopause region, *J. Geophys. Res.: Atmos*., 2003, vol. 108, no. 3, pp. 1–12.

Translated by I. Ptashnik